Published in final edited form as:

Acta Biomater. 2018 February ; 67: 111–121. doi:10.1016/j.actbio.2017.12.001.

Fabrication of hybrid crosslinked network with buffering capabilities and autonomous strengthening characteristics for dental adhesives

Linyong Song[a], **Qiang Ye**[a,*], **Xueping Ge**[a], **Anil Misra**[a,b], **Candan Tamerler**[a,c], and **Paulette Spencer**[a,c,*]

[a]University of Kansas, Institute for Bioengineering Research, 1530 W. 15th Street, Lawrence, KS 66045-7609, USA

[b]University of Kansas, Department of Civil Engineering, 1530 W. 15th Street, Lawrence, KS 66045-7609, USA

[c]University of Kansas, Department of Mechanical Engineering, 1530 W. 15th Street, Lawrence, KS 66045-7609, USA

Abstract

Ingress of bacteria and fluids at the interfacial gaps between the restorative composite biomaterial and the tooth structure contribute to recurrent decay and failure of the composite restoration. The inability of the material to increase the pH at the composite/tooth interface facilitates the outgrowth of bacteria. Neutralizing the microenvironment at the tooth/composite interface offers promise for reducing the damage provoked by cariogenic and aciduric bacteria. We address this problem by designing a dental adhesive composed of hybrid network to provide buffering and autonomous strengthening simultaneously. Two amino functional silanes, 2-hydroxy-3-morpholinopropyl (3-(triethoxysilyl)propyl) carbamate and 2-hydroxy-3-morpholinopropyl (3-(trimethoxysilyl)propyl) carbamate were synthesized and used as co-monomers. Combining free radical initiated polymerization (polymethacrylate-based network) and photoacid-induced sol-gel reaction (polysiloxane) results in the hybrid network formation. Resulting formulations were characterized with regard to real-time photo-polymerization, water sorption, leached species, neutralization, and mechanical properties. Results from real-time FTIR spectroscopic studies indicated that ethoxy was less reactive than methoxy substituent. The neutralization results demonstrated that the methoxy-containing adhesives have acute and delayed buffering capabilities. The mechanical properties of synthetic copolymers tested in dry conditions were improved via condensation reaction of the hydrolyzed organosilanes. The leaching from methoxy containing copolymers was significantly reduced. The sol-gel reaction provided a chronic and persistent reaction in wet condition-performance that offers potential for reducing secondary decay and increasing the functional lifetime of dental adhesives.

*Corresponding authors at: The University of Kansas, Institute for Bioengineering Research, School of Engineering, Learned Hall 5109, 1530 W. 15th Street, Lawrence, KS 66045-7609, USA (Q. Ye). The University of Kansas, Dept. Mechanical Engineering, School of Engineering, 1530 W. 15th Street, Lawrence, KS 66045-7609, USA (P. Spencer). yeq@ku.edu (Q. Ye), pspencer@ku.edu (P. Spencer).

Appendix A. Supplementary data

Supplementary data associated with this article can be found, in the online version, at https://doi.org/10.1016/j.actbio.2017.12.001.

Keywords

Organosilane; Dental adhesive; Photoacid-induced sol-gel reaction; Neutralization; Dynamic mechanical analysis; Self-strengthening; Composite restoration

1. Introduction

Resin-based dental composite is the most widely used material for direct restorative dentistry [1–3]. In spite of this popularity, posterior composite restorations do not characteristically provide the durability associated with dental amalgam [4,5]. The primary reason that amalgam and composite restorations fail is recurrent decay, i.e. decay on the margins of existing restorations, but recurrent decay is 3.5 times greater for composite [6–12].

A clear difference between amalgam and composite is corrosion-the corrosion products seal defects at the tooth/amalgam interface but composite materials do not corrode. The adhesive that is used to bond the composite to the tooth is intended to seal discrepancies at the composite/tooth interface, but methacrylate-based dental adhesives/composites are vulnerable to hydrolytic and enzymatic degradation [4,13–16]. This degradation leads to gaps at the interface between the composite and tooth [17,18].

Another determining factor related to the failure of composite restorations is associated with bacterial adhesion and growth at the restorative material/tooth interface. *Streptococcus mutans* (*S. mutans*) is a gram-positive, facultative anaerobic microorganism that has been implicated as the major causative agent of dental caries [19–21]. Adhesion of *S. mutans* to the material/tooth interface creates an environment that supports the subsequent attachment and growth of other bacterial species, ultimately this activity leads to a micro-ecosystem known as a biofilm. In addition to its role as a “pioneer” organism in biofilm formation, *S. mutans* produces lactic acid; the lactic acid damages the adjacent tooth surface by demineralization [22]. With the degradation of dental adhesive and the formation of biofilm on the surface of restorative materials, enzymes, oral fluids and bacteria permeate the interfacial defects, undermining the composite restoration and bacteria destroy the adjacent tooth structure [23,24].

Various strategies have been developed to prevent or slow down the degradation of dental adhesives/composites [25–27]. However, due to the inherent water-absorption of methacrylate-based synthetic biomaterials, the degradation process in the oral environment is unavoidable and irreversible [4,13,28,29]. At the same time, the inability of the material to increase the pH at the composite/tooth interface facilitates the outgrowth of more cariogenic and aciduric bacteria [30–32]. Research has shown that successful restorative treatment does not alter the numbers of *S. mutans* [20,33]. Therefore, more effective methods for reducing the cariogenic challenge at the tooth/composite interface are needed. Materials that could neutralize the micro-environment at the tooth/composite interface offer the potential of protecting tooth structure and reducing the negative impact of bacteria at the margins of composite restorations [30]. With the emphasis on less invasive operative techniques, there is

a pressing need to develop functionalized dental adhesives/composites capable of neutralization [34–36], bioactivity [37–39], or mineralization [40–42].

In our previous work, 2-N-morpholinoethyl methacrylate (MEMA) as amine-containing monomer ($pK_a = 6.2$) has been used to develop dental adhesive with neutralization capability [34]. MEMA-containing resin formulations showed good storage stability and MEMA-based copolymers showed low toxicity when used as a controlled drug-delivery system [43–45]. However, MEMA-functionalized copolymers showed fast neutralization behavior when loosely crosslinked network was formed, which would potentially limit the long-term performance of these materials under clinical conditions. Recently, we have developed a self-strengthening dental adhesive by introducing photoacid-induced sol-gel reaction together with the free radical photo-polymerization of methacrylate [46,47]. The results indicated that whether in wet conditions (pH ~ 5.5 @25 °C) or in acidic conditions (pH ≤ 3.5 @25 °C), the sol-gel reaction is a suitable and novel approach to enhance the mechanical properties of the newly developed dental adhesive copolymers [46,47].

In this study, two amino functional alkoxysilanes were synthesized and incorporated in a dental adhesive formulation to provide a hybrid material with neutralization capabilities and self-strengthening characteristics. We first evaluated the effect of different alkoxy groups of silane on the hydrolysis/condensation of the sol-gel reaction. We next investigated the neutralization behavior and mechanical properties of the hybrid copolymers following prolonged aqueous storage. The present study tests the hypothesis that: i) the amine group built-in to the dental adhesive network by photoacid-induced sol-gel reaction can neutralize lactic acid, and ii) the mechanical properties of dental adhesive can be improved in wet conditions. By combining neutralization capacity and self-strengthening characteristics, the developed hybrid copolymers are postulated to serve as dental adhesives that provide better long-term performance in the oral environment.

2. Materials & methods

2.1. Materials

2,2-Bis[4-(2-hydroxy-3-methacryloxypropoxy) phenyl]propane (BisGMA), 2-hydroxyethyl methacrylate (HEMA), camphoroquinone (CQ), ethyl-4-(dimethylamino) benzoate (EDMAB), diphenyliodonium hexafluorophosphate (DPIHP), L(+)-lactic acid (LA), dibutyltin dilaurate (DBTL), 3-morpholino-1,2-propanediolb (MPD), and (3-isocyanatopropyl) triethoxysilane (IPTES), were obtained from Sigma-Aldrich (St. Louis, MO) and used as received without further purification. (3-isocyanatopropyl) trimethoxysilane (IPTMS, 95%) was purchased from Gelest Inc., (Morrisville, PA). 2-hydroxy-3-morpholinopropyl (3-(triethoxysilyl)propyl) carbamate (SNE), 2-hydroxy-3-morpholinopropyl (3- (trimethoxysilyl)propyl) carbamate (SNM) were synthesized in our laboratory and used as co-monomers (see SI Scheme 1). All other chemicals were used as received without further purification.

2.2. Synthesis of co-monomer SNE/SNM

The new co-monomers, SNE/SNM, were synthesized based on the following procedures [48]. Briefly, to a 250–mL, round bottom flask, fitted with a magnetic stirrer and N_2–purging, MPD (4.20 g, 25 mmol), DBTL (20 μL) and tetrahydrofuran (THF, 50 mL) were added. When the temperature was cooled to 0 °C with an ice-water bath, IPTES (6.38 g, 25 mmol, for SNE) or IPTMS (5.13 g, 25 mmol, for SNM) dissolved in 40 mL THF was added stepwise over a 2 h period. Next, the reaction mixture was kept at 0 °C for 4 h and raised to 23 ± 2 °C for another 20 h. The progress of the reaction was followed by FTIR (Spectrum 400 Fourier transform infrared spectrophotometer, Perkin-Elmer, Waltham, MA) to monitor the disappearance of isocyanate (_NCO) at 2266 cm^{-1}. After the reaction was completed, THF was removed by rotary evaporation and ethyl acetate (100 mL) was added to dissolve residual liquid. Then 100 mL saturated NaCl solution was added to wash the unreacted starting materials. The EA oil-phase was dried over anhydrous $MgSO_4$ and followed by removing the solvent with a rotary evaporator at 40 °C to obtain as colorless oil SNE (7.65 g, 75% theory). THF was removed from SNM after the reaction was completed by rotary evaporation to obtain viscous colorless oil (8.06 g, 88% theory).

2.3. Preparation of adhesive formulations

Neat methacrylate resin made by mixing 45 wt% HEMA and 55 wt% BisGMA was used as the control (C0) [15]. CQ (0.5 wt%), EDMAB (0.5 wt%), and DPIHP (0.5 wt%) were used as 3-component photoinitiators (PIs) system [49–51] with respect to the total amount of monomers. The composition of the neat resin and the experimental resin formulations are listed in Table 1. Mixtures of the monomers/PIs were prepared in brown glass vials under amber light. The preparation of adhesive formulations and their polymer beams have been reported [49,50].

2.4. Water miscibility of adhesive formulations

The protocol for determining water miscibility of adhesive formulations has been reported in detail [52,53]. In brief, about 0.5 g of each neat resin was weighed into a brown vial with water added in increments of approximately 0.005 g until the mixture was visually observed to be turbid. The percentage of water in the mixture was noted (w_1). The mixture was then back-titrated using the neat resin until the turbidity disappeared, and the percentage of water in the mixture was noted (w_2). Then the water miscibility (W_{wm}, %) of the liquid formulation was calculated as the average of w_1 and w_2. Three specimens of each formulation were measured.

2.5. Specimens preparation

The prepared resins were injected into a glass-tubing mold (Fiber Optic Center, Inc., part no.: ST8100, New Bedford, MA) and light-cured for 40 s at 23 ± 2 °C with an LED light curing unit (LED Curebox, 100 mW/cm^2 irradiance, Proto-tech, Portland, OR). The polymerized samples were stored in the dark at 23 ± 2 °C for at least 48 h before being used. The resultant rectangular beam specimens of cross section 1 mm × 1 mm and length 15 mm were used to determine the dynamic mechanical properties.

2.6. Real-time conversion and maximum polymerization rate

The degree of conversion (DC) and polymerization behavior were determined by FTIR as reported [47]. A time-based spectrum collector (Spectrum TimeBase, Perkin-Elmer) was used for continuous and automatic collection of spectra during polymerization. A minimum of three measurements were carried out for each adhesive formulation. Methacrylic double bond conversion was monitored by the band ratio profile-1637 cm^{-1} (C=C)/1608 cm^{-1} (phenyl). The maximum polymerization rate ($R_p^{max}/[M]$) was determined using the maximum slope of the linear region of the DC vs. time plot [50,54,55].

2.7. Dynamic mechanical analysis (DMA)

In the current study, DMA tests were performed using a TA instruments Q800 DMA (TA Instruments, New Castle, USA) with a three-point bending clamp. The dynamic mechanical properties of polymethacrylate-based dental adhesives have been described [49,56]. Rectangular beam specimens were used for DMA measurements and a minimum of three specimens were tested for each formulation. For dry testing, the following testing parameters were used: displacement amplitude of 15 μm, frequency of 1 Hz and preload force of 0.01 N [57]. In addition to this, temperature was ramped at the rate of 3 °C/min from 20 to 200 °C. For wet testing, specimens were first submerged in 1 M LA solution at 37 °C for 4 or 8 weeks with tests being obtained using the three-point submersion clamp [54]. The test temperature was varied from 10 to 75 °C with a ramping rate of 1.5 °C/min.

2.8. Neutralization measurements

The neutralization measurements for both dry and hydrated samples were performed with a Mettler Toledo (Columbus, OH) Accument® AP110 pH meter equipped with a micro-probe. Dry disc specimens (~20 mg) were soaked directly in the lactic acid (LA) solution (1 mM, 2 mL). For the hydrated samples, prior to the neutralization experiment, the disc specimens (~20 mg) were prewashed in water at 37 °C for 7 days. Then, the hydrated specimens were soaked in the LA solution (1 mM, 2 mL). The pH values of solution were measured at fixed time intervals. A minimum of four specimens for each formulation were measured.

2.9. Leachable study by high-performance liquid chromatography (HPLC)

Round disc samples (~4 mm diameter and ~1.2 mm thickness) were used for the leachable study [46,58]. Two disc samples were soaked in 2 mL ethanol (HPLC grade) at 23 ± 2 °C for 1 to 56 days. The storage solutions were collected at various time intervals, i.e. 1, 2, 4, 7, 10, 14 days and every week after the 14-day time point. Fresh ethanol was added after each collection. The concentration of leachate in the collected storage solutions was determined using high performance liquid chromatography (HPLC). HPLC analysis was completed using a system (Shimadzur® LC-2010C HT, software EZstart, version 7.4 SP2) equipped with a 250 × 4.6 mm column packed with 5 μm C-18 silica (Luna®, Phenomenex Inc., Torrance, CA) under the following conditions: mobile phase made with acetonitrile/water (70/30, v/v); 0.5 mL/min flow rate; 20 μL sampling loop; UV detection at 208 nm; 40 °C column temperature. The column was calibrated with known concentrations of compounds, e.g., HEMA and BisGMA ethanol solutions. The calibration curves with the linear fittings of BisGMA (5–250 mg/L, $R^2 = 0.999$) and HEMA (5–500 mg/L, $R^2 = 0.999$), were used to

calculate the concentration of each monomer in the eluent based on the intensity of the chromatographic peaks at the corresponding retention times.

2.10. Statistical analysis

The results (degree of conversion measured by FTIR, rubbery moduli and glass transition temperature values obtained from DMA) were analyzed statistically using one-way analysis of variance (ANOVA), together with Tukey's test at $\alpha = 0.05$ (Microcal Origin Version 8.0, Microcal Software Inc., Northampton, MA) to identify significant differences in the means.

3. Results

3.1. Water miscibility

We first test the water miscibility of the experimental and control adhesives at 23 ± 2 °C (Table 1). The water miscibility (W_{wm}) of the control (C0), which is used as a commercial analog, is recorded as 10.5 ± 0.1%. When we increased the SNE (2-hydroxy-3-morpholinopropyl (3-(triethoxysilyl)propyl) carbamate) concentrations from 5, 10, 15, 20, 35, to 50 wt%, the W_{wm} increased from 10.8 ± 0.1, 11.1 ± 0.1, 11.3 ± 0.1, 11.5 ± 0.0, 12.5 ± 0.1, to 14.2 ± 0.0 wt%, respectively. With increasing SNM (2-hydroxy-3-morpholinopropyl (3-(trimethoxysilyl)propyl) carbamate) concentration from 5, 10, 15, to 20 wt%, the W_{wm} increased from 10.5 ± 0.2, 10.7 ± 0.3, 11.0 ± 0.1, to 11.4 ± 0.2 wt%, respectively.

3.2. Polymerization kinetic

Real-time photo-polymerization behavior of the C0 and experimental adhesives is shown in Fig. 1 (A and B). The experimental formulations that contain SNE or SNM co-monomers, exhibit significantly higher DC than that of the C0 ($p < .05$). The maximum polymerization rates ($R_p^{max}/[M]$) of the experimental formulations were higher than that of the C0, and reached the highest values when the SNE or SNM concentration was 10 wt% (results see Table 1). Fig. 1C and D show the characteristic peaks of FTIR spectra of SNE-containing adhesive formulation (HBSN-50) at different times after visible-light irradiation. In the C—H stretching region, the intensity of the band at 2972, 2928, and 2880 cm^{-1} remained constant over 8 h. At the same time, the intensity of the broad band at 340 cm^{-1} (hydrogen bonded OH stretching mode) was almost unchanged. This result indicated that even over 8 h, the hydrolysis of ethoxy group is barely observable after visible light-irradiation is terminated.

3.3. Neutralization

The pH of LA solution, as a function of storage time, for the non-prewashed/prewashed control or experimental copolymer specimens is shown in Fig. 2. Whether the C0 is non-prewashed or prewashed in water, the pH values of LA solution increased from 3.5 to about 3.8 and finally equilibrated at 4.0–4.2. When the non-prewashed HBSN or HBSM specimens were soaked in the LA solution, the pH values increased at different levels according to the SNE/SNM concentration. When alkoxysilane monomer was at a higher concentration (SNE is 35 or 50 wt%, SNM is 20 wt%), the pH value rapidly increased and

reached a plateau within several days. When SNE/SNM concentration was lower than 20 wt %, the pH values slowly increased and took 4–6 weeks to reach a plateau. When the prewashed HBSM specimens were soaked into LA solution, the pH values increased from 3.5 to about 3.8, and then slowly increased with storage time. When SNM is 20 wt%, the pH value took about 6 weeks to reach equilibrium at about 6.0, which is lower than that of non-prewashed specimen at equilibrium (about 6.7). Compared with the results obtained from non-prewashed experimental specimens, there was a significant increase in the time required to reach equilibrium.

3.4. Mechanical properties in dry and wet conditions

The dynamic mechanical properties of the SNM-containing copolymers in dry conditions and tested at various temperatures are shown in Fig. 3. Two cycles of temperature-ramp analysis up to 200 °C were run for these specimens. In the first cycle, with the increase of SNM concentration, the rubbery moduli for the experimental copolymers were comparable (SNM = 5 wt%) or significantly higher than that of the C0 ($p < .05$). However, T_g values determined by the tan δ peak of the experimental were significantly lower than that of the C0 ($p < .05$). The storage modulus at 37 °C, rubbery modulus, and the T_g of the C0 obtained in the second DMA cycle were comparable with that measured in the first cycle. However, corresponding values of the experimental specimens in second cycle were significantly higher than that in the first cycle ($p < .05$, details are shown in SI Table 1).

Fig. 4 shows the mechanical properties of the C0 and the SNM-containing experimental specimens stored in 1 M LA for 4 or 8 weeks. With the increase in storage time from 4 to 8 weeks, the storage moduli of the C0 and the experimental specimens at 37 °C did not show significant dependence on the storage time. The moduli at 37 °C of the experimental specimens were significantly lower than that of the C0 ($p < .05$) whether they were soaked for 4 or 8 weeks. In contrast, the T_g of HBSM-20 specimen soaked over 8 weeks was significantly higher than that of the C0 ($p < .05$).

3.5. HPLC results

Fig. 5 shows the results of cumulative monomers released from the SNM-containing copolymers as a function of incubation time in ethanol for 8 weeks at 23 ± 2 °C. With the increase of SNM concentration from 0, 5, 10, 15, and to 20 wt% in the formulations, the cumulative release of HEMA decreased from 1107, 924, 631, 420, to 292 μg/mL, and the percentage of leached HEMA based on the total HEMA used in the corresponding adhesive formulation decreased from 12.0, 10.4, 7.6, 5.4, to 4.0 wt% (calculated method see SI); the cumulative release of BisGMA decreased from 549, 486, 411, 372, and to 349 μg/mL, and the percentage of leached BisGMA slightly decreased from 4.9, 4.5, 4.0 to 3.8 wt%.

4. Discussion

4.1. Effects of alkoxy substituent

In our previous study, an autonomic, self-strengthening, Si-based (γ-methacryloxyproyl trimethoxysilane, MPS) hybrid system was developed for potential application as a dental adhesive [47]. The methoxy groups of MPS are hydrolyzed to form silanol-containing

species, which are highly reactive intermediates and can generate Si—O—Si or Si—O—C covalent bonds. In the current study, we investigated the reactivity of alkoxy substituent in organosilane during visible light-induced photo-polymerization. Usually the reaction rate of acid-catalyzed hydrolysis of organosilane is significantly greater than that of the base-catalyzed hydrolysis [59], and is minimally affected by other carbon-bonded substituents. The hydrolysis is preceded by protonation of the alkoxy groups and the hydrolysis rates of alkoxy groups are generally related to their steric bulk, such as $CH_3O > C_2H_5O$ [59,60], a methoxysilane hydrolyzed at 6–10 times the rate of an ethoxysilane. In the previous MPS study, the degree of hydrolysis of methoxysilane was found to be ~50% within 8 h [47]. From the real-time FTIR spectroscopic study (Fig. 1C and D), it can be observed that the intensity of the characteristic peak of SNE-containing specimens remained constant, which indicated that the hydrolysis of ethoxy group was too slow to be observed during the limited time scale of this investigation. At the same time, with the increase of SNE concentration from 5, 10, 15, 20, 35, to 50 wt% in the formulations, the weight loss of copolymer specimens soaked in water for 7 days increased from 2.0 ± 0.1, 2.8 ± 0.3, 3.9 ± 0.1, 5.5 ± 0.1, 12.9 ± 0.2, to 32.6 ± 1.2%. These results indicate that most of the SNE was gradually leached from the specimens. Meanwhile, with the increase of SNM concentration from 5, 10,15, to 20 wt%, the weight losses increased from 1.8 ± 0.2, 2.9 ± 0.1, 4.6 ± 0.2, to 6.2 ± 0.1%, which were comparable or slightly higher than the SNE-containing specimens. This phenomenon was mainly attributed to the faster hydrolysis rate of methoxy group as compared to the ethoxy group. The FT-IR result indicates that none of ethoxy functional groups (SNE-containing samples) could be hydrolyzed. Meanwhile, the methoxy groups (SNM-containing specimens) could be hydrolyzed and the copolymers became more hydrophilic with the increase of silanol groups [46,47]. The complicated pathway for hydrolysis and condensation of SNM has inhibited our ability to simultaneously determine the kinetics of silanol formation and reaction. Due to the limited condensation reaction of silanol groups in the highly crosslinked polymethacrylate-based network, part of the hydrolyzed SNM may tend to leach during aging in aqueous solution.

4.2. Neutralization behavior

The results related to the buffering potential of the non-prewashed/prewashed copolymer specimens are presented in Fig. 2. With the control formulation, whether the non-prewashed or prewashed specimens, the pH values of the LA solution are similar, i.e. about 4.0–4.2 after 9 weeks. When the non-prewashed SNE-containing copolymer specimens were soaked in LA solution, the pH values showed a gradually increasing trend, except in the case of higher SNE concentrations (35 and 50 wt%), where an acute change in pH occurred. The acute neutralization response to the HBSN-35/50 specimens could be attributed to release of the SNE monomer from the specimens. The weight loss of the HBSN-35/50 specimens was 12.9 ± 0.2 and 32.6 ± 1.2%, which was significantly higher than that of the control (1.5 ± 0.2%). The higher weight loss is likely related to leaching of the SNE co-monomer. When the SNE concentration was varied from 5 to 20 wt%, the pH values increased gradually and exhibited an increasing trend after 9 weeks. There are two primary reasons for these results. First, SNE co-monomer could be leached since it cannot be polymerized into the network structure via the relatively slow sol-gel reaction. Second, due to the highly crosslinked and dense polymethacrylate-based network structure, it could take much longer for the entrapped

SNE molecules to diffuse out and for the protons to diffuse into the polymer, which may depress the neutralization behavior.

When the non-prewashed SNM-containing specimens were soaked into the LA solution, the pH showed a similar trend with that of the SNE-containing samples. The difference was the neutralization rate with the SNM-containing samples was relatively fast as compared to the SNE-containing samples. When the SNM/SNE concentration was 20 wt% in the formulation (HBSM-20 or HBSE-20, Fig. 2A and B), the pH value reached equilibrium after 3–4 weeks for the HBSM-20 sample, however, it is almost 9 weeks for the HBSN sample. These results are likely due to the difference in reactivity of SNM and SNE co-monomer. Most of the methoxy groups could be hydrolyzed to generate silanol groups after the light-cured specimen was stored for 48 h in the dark. When the SNM-containing specimens were soaked in the LA solution, the hydrolyzed SNM molecules became more hydrophilic and preferred to diffuse out, thus quickly neutralizing the acid. In contrast, due to the less reactivity and increased hydrophobicity of the ethoxy group, it took longer for the SNE monomer to be hydrolyzed and leached from the polymer.

It has been reported that the higher localized pH (around 6.0– 6.5) could inhibit the growth of aciduric organisms, such as *S. mutans* [61]. Furthermore, with the fluctuations in pH that occur *in vivo*, fast neutralization of tooth restoration materials would be beneficial under clinical conditions [32,61]. To date, most of the buffering function was provided by the decomposition or ion releasing compounds [35,40,61,62]. Biomaterials that achieve buffering via leaching of ions typically provide this capability for a relatively short time (hours to days) and may experience a gradual deterioration of physical properties.

In our previous study, amine-functionalized co-monomers have been introduced into the dental adhesive resin and the copolymers showed a long-term neutralization capacity [34,53,63,64]. In the present work, with the incorporation of amine functionalized polymerizable component (SNM), the copolymers showed promising neutralization capacity, which could offer the benefit of maintaining the neutral pH at the localized microenvironment of the restorative material/tooth interface. Therefore, the hypothesis (i) that the amine group built-in to the dental adhesive network by photoacid-induced sol-gel reaction can neutralize acid, was accepted.

4.3. Mechanical properties

Dynamic mechanical analysis (DMA) is suitable to characterize the viscoelastic behavior of materials and has been suggested as a valuable tool for obtaining information such as crosslinking density and heterogeneity of polymer networks [65,66].

With the increase of the SNM concentration in the formulations (Fig. 3), the rubbery moduli of the experimental in dry condition were significantly higher than that of the C0 ($p < .05$), which indicated that a higher crosslink network was obtained with the addition of SNM. However, the rubbery moduli of SNE-containing specimens were significantly lower than that of the C0 ($p < .05$), except for HBSN-5 (See SI Fig. 3A). These results indicated that the more reactive SNM improved the crosslink density of the hybrid polymer network. Meanwhile, it was observed that the T_g of experimental copolymers, such as HBSM-20

(118.5 ± 1.2 °C) was significantly lower than that of C0 (149.0 ± 0.7 °C). This phenomenon could be attributed primarily to the plasticization of the hydrolyzed SNM. The same trend was observed in the SNE-containing samples (See SI Fig. 3C).

One of the advantages of photopolymerization is that it can be carried out at room temperature. Nevertheless, due to the relatively slow reaction rate of the sol-gel reaction, when the liquid resin is irradiated by visible-light, a polymethacrylate-based matrix network is formed by simultaneous free radical cross-linking polymerization of methacrylate monomers while the alkoxysilane shows limited hydrolysis and condensation. As mentioned above, the condensation reaction of the silane was very limited in the highly crosslinked polymethacrylate-based network. In the present study, the heated samples (done by first DMA cycle –ramp from 20 °C up to 200 °C) were run for a second time to verify the effect of the condensation reaction. In the first DMA cycle, the samples were heated up to 200 °C, which was above the T_g of copolymers. The mobility of the polymer chains at high temperature was significantly improved, thus the condensation reaction would be promoted and the crosslink density of hybrid network should be improved, as evident from the results of the secondary DMA cycle.

When the SNE/SNM-containing specimens were run under DMA testing for a second cycle, the storage moduli at the rubbery region were improved significantly as compared to that of the first cycle (see Fig. 3C and SI Table 1). These results further confirmed that the limited sol-gel reaction occurred after the visible light irradiation and can be promoted by heating processes. At the same time, it can be observed that the T_g values of the control were similar in the first and second cycles, which indicated that the further free radical polymerization was very limited and that there was minimal change in the polymethacrylate-based network structure during the heating process. In comparison, the T_g values of the SNM-containing specimens were improved about 8–22 °C in the second cycle. Due to the fast rate of free radical polymerization, the transition from liquid to solid state in the resin occurs within a couple of seconds. With the formation of the polymethacrylate-based matrix, the mobility of the polymer chains and functional groups ($-SiOCH_3$) were restrained, which depressed the further free radical polymerization to the un-reacted C=C bond, and also the sol-gel reaction (hydrolysis and condensation). When the sample was heated during the first DMA cycle, the mobility of the copolymer chains was significantly enhanced, especially at the rubbery region. Therefore the further free radical polymerization and the sol-gel reaction were promoted. Our previous study showed that the degree of hydrolysis of methoxysilyl groups can reach at ~70% after the visible light-irradiation is terminated and the specimen is stored for 48 h [47]. During the heating process in the first DMA cycle, the condensation reactions between silanol-silanol, silanol-methoxy or silanol-hydroxyl were prompted and highly crosslinked hybrid networks were obtained. Therefore, the significant increase of T_g values of the SNM/SNE-containing specimens was observed.

The three-point bending submersion clamp method is expected to simulate the wet environment of the mouth. The storage moduli of the C0 and experimental samples were significantly lower than those of the dry samples. The difference is caused by water plasticization. The water miscibility of the experimental formulation was higher than that of the C0. This means that the experimental formulation was more hydrophilic than that of the

C0 and thus, the experimental specimens were able to absorb more water. With the extension of storage time from 4 to 8 weeks in LA solution, whether the C0 or the experimental samples, the storage modulus at 37 °C showed a slight increase. However, the T_g values of the experimental samples showed a significant increase when the SNM concentration was 15 and 20 wt%. This result was attributed to the further crosslinking reaction (*via* the condensation reaction between silanol/silanol or silanol/hydroxyl groups) in a wet condition. As a results, the hypothesis (ii) that the mechanical properties of dental adhesive can be improved in wet conditions, was accepted.

A schematic illustration of the hybrid network formation after visible-light irradiation is given in Scheme 1. FTIR results have confirmed the free radical polymerization rate is much faster than that of the photoacid-catalyzed sol-gel reaction [47]. When the liquid resin is irradiated by visible-light, the polymethacrylate-based network is formed first by free radical polymerization of co-monomers, e.g., HEMA and BisGMA. Simultaneously, the methoxysilyl groups of SNM are hydrolyzed, which is catalyzed by the photoacid (Brønsted acid, $H^+PF_6^-$) produced during the visible-light irradiation [67–69]. Our previous studies have shown that the degree of hydrolysis and condensation of methoxysilyl group is very limited (<5%) during 40 s visible-light irradiation, and the newly formed Si–O–Si bonds are limited even after 24 h post curing [46,47]. The increased rubbery moduli obtained from the DMA in dry condition (secondary cycle) supported this proposed mechanism. During the heating process, the increased mobility of polymer chains promote the condensation reactions, which contribute to the highly crosslinked network. However, due to the mono-type functional group of SNM and the relatively slow rate of condensation reactions, partial SNM or low molecular weight oligomer tend to leach when soaked in water, which accounts for the acute neutralization phenomenon (Fig. 2B). Meanwhile, most of the SNM has been trapped into the polymethacrylate-based network and grafted onto the polymer chains via sol-gel reaction, which contributes to the delayed neutralization behavior (Fig. 2C).

4.4. Leaching properties

To accelerate the diffusion of the hydrophobic compounds, i.e., BisGMA and EDMAB from the copolymers, ethanol was used as the solvent for the leaching study. With the increase of SNM concentration, the amount of HEMA and BisGMA that was leached decreased significantly. As reported previously [47] the main reason was the further crosslinked network formed through the condensation reactions between silanol/silanol or silanol/hydroxyl groups. With the addition of 20 wt% SNM in the formulation, the cumulative amounts of leached HEMA and BisGMA were reduced by about 68 and 22%, respectively. Due to the lack of UV absorption, it is hard to determine the leaching behavior of SNM co-monomer by HPLC. From the weight loss result (see SI Fig. 2), it can be roughly estimated that the percentage of leached SNM was about 20%. This result was significantly higher than the MPS-containing copolymers (percentage of leached MPS to total MPS in the formulation was less than 3%) [47]. The main difference between SNM and MPS was the functionality. MPS has two types of functional groups, i.e., the methacrylate C=C bond and the methoxysilyl group. However, SNM has only a methoxysilyl functional group. During the light-irradiation, the dual functional MPS can be copolymerized with HEMA/BisGMA via free radical polymerization and polymerized into the network via sol-gel reaction. Due to

the relatively slow rate of the sol-gel reaction, even stored in dark for 2 days, there is still a lot of un-polymerized SNM or low-molecular-weight oligomers. Consequentially, the amount of leached SNM was significantly higher than that of MPS. Meanwhile, the release rates of HEMA or BisGMA in the experimental samples in this study were depressed, which could be attributed to the higher crosslink density network formed through the hetero-condensation between silanol and hydroxyl groups.

It must be noted that the immersing media, ethanol, is not a clinically relevant solvent. We used ethanol to accelerate the leachable study. Due to the good solubility and compatibility of ethanol, the concentration of the leached HEMA plateaued within 14 days. However, the concentration of the leached BisGMA has not plateaued even after 56 days. When considering the oral aqueous environment, hydrophilic component, HEMA, in the polymer would be the major leachable. All in all, HPLC data obtained from specimens stored in ethanol would be expected to yield a higher cumulative concentration of leachates as compared to clinical conditions and therefore the results should be interpreted with caution.

The significantly reduced leachate amounts in SNM-containing copolymers indicated that the experimental adhesive could maintain the integrity of the network structure. These promising results suggest a design strategy for biocompatible dental adhesive with improved durability and lower toxicity. Future work will focus on improving the mechanical properties and minimizing the leachable species by exploring the structure-property relationships of the developed hybrid biomaterial. The potential for buffering the local environment and the autonomic self-strengthening characteristics could offer a more durable adhesive and a concomitant improvement in the lifetime of composite restorations. Our attempt towards the establishment of structure-property-function relationships in the hybrid system could promote the development of next-generation dental restorative products. At the same time, it is tempting to speculate the advantages that the developed hybrid system could offer additional applications beyond dental restorations, including their use as wound/postoperative sealing materials and developing gradient interfaces at the implantable material tissue interfaces [70–72].

5. Conclusion

We designed a dental adhesive composed of hybrid network that can simultaneously provide buffering capabilities and autonomous strengthening characteristics. The amino functional organosilane monomers showed potential application in developing dental adhesive with neutralization capability. The ethoxy substituent showed relative lower reactivity than methoxy during and after the visible light-irradiation. The higher reactivity of methoxy groups led to more hydrophilic silanol species, which promoted the diffusion and condensation of SNM and provided acute and delayed neutralization. Dynamic mechanical analysis, carried out in dry condition, indicated that the condensation reaction could be promoted at high temperatures resulting in more densely cross-linked hybrid networks. The persistently improved mechanical properties of copolymers in wet conditions indicated that the photoacid-induced sol-gel reaction could strengthen these biomaterials in the oral environment. The HPLC results indicated that the cumulative amounts of unreacted HEMA and BisGMA were reduced significantly from the SNM-containing copolymers. The SNE/

SNM-containing copolymers showed a fast neutralization rate at much higher concentrations; this finding demonstrates the significant potential of this approach for providing buffering capacity in the hybrid dental adhesive.

Supplementary Material

Refer to Web version on PubMed Central for supplementary material.

Acknowledgments

This investigation was supported by research grants R01DE022054, 3R01DE022054-04S1 and R01DE025476 from the National Institute of Dental and Craniofacial Research, National Institutes of Health, Bethesda, Maryland. The authors declare no potential conflicts of interest with respect to the authorship and/or publication of this article.

References

1. Delaviz Y, Finer Y, Santerre JP. Biodegradation of resin composites and adhesives by oral bacteria and saliva: a rationale for new material designs that consider the clinical environment and treatment challenges. Dent. Mater. 2014; 30:16–32. [PubMed: 24113132]
2. Cramer NB, Stansbury JW, Bowman CN. Recent advances and developments in composite dental restorative materials. J. Dent. Res. 2011; 90:402–416. [PubMed: 20924063]
3. Moszner N, Hirt T. New polymer-chemical developments in clinical dental polymer materials: Enamel-dentin adhesives and restorative composites. J. Polym. Sci. Pol. Chem. 2012; 50:4369–4402.
4. Santerre JP, Shajii L, Leung BW. Relation of dental composite formulations to their degradation and the release of hydrolyzed polymeric-resin-derived products. Crit. Rev. Oral Biol. M. 2001; 12:136–151. [PubMed: 11345524]
5. Opdam NJM, Bronkhorst EM, Loomans BAC, Huysmans MCDNJM. 12-Year survival of composite vs. amalgam restorations. J. Dent. Res. 2010; 89:1063–1067. [PubMed: 20660797]
6. Bernardo M, Luis H, Martin MD, Leroux BG, Rue T, Leitao J, DeRouen TA. Survival and reasons for failure of amalgam versus composite posterior restorations placed in a randomized clinical trial. J. Am. Dent. Assoc. 2007; 138:775–783. [PubMed: 17545266]
7. Manhart J, Chen HY, Hamm G, Hickel R. Review of the clinical survival of direct and indirect restorations in posterior teeth of the permanent dentition. Oper. Dent. 2004; 29:481–508. [PubMed: 15470871]
8. Peumans M, Kanumilli P, De Munck J, Van Landuyt K, Lambrechts P, Van Meerbeek B. Clinical effectiveness of contemporary adhesives: a systematic review of current clinical trials. Dent. Mater. 2005; 21:864–881. [PubMed: 16009415]
9. Spencer P, Ye Q, Misra A, Goncalves SEP, Laurence JS. Proteins, pathogens, and failure at the composite-tooth interface. J. Dent. Res. 2014; 93:1243–1249. [PubMed: 25190266]
10. van de Sande FH, Collares K, Correa MB, Cenci MS, Demarco FF, Opdam NJM. Restoration survival: revisiting patients' risk factors through a systematic literature review. Oper. Dent. 2016; 41:S7–S26. [PubMed: 27689931]
11. Brouwer F, Askar H, Paris S, Schwendicke F. Detecting secondary caries lesions: a systematic review and meta-analysis. J. Dent. Res. 2016; 95:143–151. [PubMed: 26464398]
12. Nedeljkovic I, Teughels W, De Munck J, Van Meerbeek B, Van Landuyt KL. Is secondary caries with composites a material-based problem? Dent Mater. 2015; 31:E247–E277. [PubMed: 26410151]
13. Hashimoto M, Ohno H, Kaga M, Endo K, Sano H, Oguchi H. In vivo degradation of resin-dentin bonds in humans over 1 to 3 years. J. Dent. Res. 2000; 79:1385–1391. [PubMed: 10890717]
14. Amaral FLB, Colucci V, Palma-Dibb RG, Corona SAM. Assessment of in vitro methods used to promote adhesive interface degradation: a critical review. J. Esthet. Restor. Dent. 2007; 19:340–353. [PubMed: 18005284]

15. Kostoryz EL, Dharmala K, Ye Q, Wang Y, Huber J, Park JG, Snider G, Katz JL, Spencer P. Enzymatic biodegradation of HEMA/BisGMA adhesives formulated with different water content. J. Biomed. Mater. Res. Part B. 2009; 88B:394–401.
16. Park JG, Ye Q, Topp EM, Lee CH, Kostoryz EL, Misra A, Spencer P. Dynamic mechanical analysis and esterase degradation of dentin adhesives containing a branched methacrylate. J. Biomed. Mater. Res. Part B. 2009; 91B:61–70.
17. Ferracane JL, Hilton TJ. Polymerization stress – is it clinically meaningful? Dent Mater. 2016; 32:1–10. [PubMed: 26220776]
18. Li Y, Carrera C, Chen R, Li J, Lenton P, Rudney JD, Jones RS, Aparicio C, Fok A. Degradation in the dentin-composite interface subjected to multi-species biofilm challenges. Acta Biomater. 2014; 10:375–383. [PubMed: 24008178]
19. ElRahman AMA, Gregory RL, Avery DR. Effect of restorative treatment on Streptococcus mutans and IgA antibodies. J. Dent. Res. 1997; 76:734. [PubMed: 9109822]
20. Gregory RL, el-Rahman AM, Avery DR. Effect of restorative treatment on mutans streptococci and IgA antibodies. Pediatr. Dent. 1998; 20:273–277. [PubMed: 9783299]
21. Takahashi N, Nyvad B. The role of bacteria in the caries process: ecological perspectives. J. Dent. Res. 2011; 90:294–303. [PubMed: 20924061]
22. Horie K, Shimada Y, Matin K, Ikeda M, Sadr A, Sumi Y, Tagami J. Monitoring of cariogenic demineralization at the enamel-composite interface using swept-source optical coherence tomography. Dent. Mater. 2016; 32:1103–1112. [PubMed: 27427292]
23. Breschi L, Mazzoni A, Ruggeri A, Cadenaro M, Di Lenarda R, Dorigo ED. Dental adhesion review: aging and stability of the bonded interface. Dent. Mater. 2008; 24:90–101. [PubMed: 17442386]
24. Bertassoni LE, Orgel JPR, Antipova O, Swain MV. The dentin organic matrix - limitations of restorative dentistry hidden on the nanometer scale. Acta Biomater. 2012; 8:2419–2433. [PubMed: 22414619]
25. Liu Y, Tjaderhane L, Breschi L, Mazzoni A, Li N, Mao J, Pashley DH, Tay FR. Limitations in bonding to dentin and experimental strategies to prevent bond degradation. J. Dent. Res. 2011; 90:953–968. [PubMed: 21220360]
26. Tjaderhane L, Nascimento FD, Breschi L, Mazzoni A, Tersariol ILS, Geraldeli S, Tezvergil-Mutluay A, Carrilho M, Carvalho RM, Tay FR, Pashley DH. Strategies to prevent hydrolytic degradation of the hybrid layer-a review. Dent. Mater. 2013; 29:999–1011. [PubMed: 23953737]
27. Hashimoto M. A review-micromorphological evidence of degradation in resin-dentin bonds and potential preventional solutions. J. Biomed. Mater. Res. Part B. 2010; 92B:268–280.
28. Gopferich A. Mechanisms of polymer degradation and erosion. Biomaterials. 1996; 17:103–114. [PubMed: 8624387]
29. Finer Y, Santerre JP. Salivary esterase activity and its association with the biodegradation of dental composites. J. Dent. Res. 2004; 83:22–26. [PubMed: 14691108]
30. Thomas RZ, van der Mei HC, van der Veen MH, de Soet JJ, Huysmans MCDNJM. Bacterial composition and red fluorescence of plaque in relation to primary and secondary caries next to composite: an in situ study. Oral Microbiol. Immun. 2008; 23:7–13.
31. Carvalho RM, Manso AP, Geraldeli S, Tay FR, Pashley DH. Durability of bonds and clinical success of adhesive restorations. Dent. Mater. 2012; 28:72–86. [PubMed: 22192252]
32. Nedeljkovic I, De Munck J, Slomka V, Van Meerbeek B, Teughels W, Van Landuyt KL. Lack of buffering by composites promotes shift to more cariogenic bacteria. J. Dent. Res. 2016; 95:875–881. [PubMed: 27146702]
33. Petti S, Pezzi R, Cattaruzza MS, Osborn JF, DArca AS. Restoration related salivary Streptococcus mutans level: a dental caries risk factor? J Dent. 1997; 25:257–262. [PubMed: 9175355]
34. Song LY, Ye Q, Ge XP, Spencer P. Compositional design and optimization of dentin adhesive with neutralization capability. J. Dent. 2015; 43:1132–1139. [PubMed: 26144189]
35. Madruga FC, Ogliari FA, Ramos TS, Bueno M, Moraes RR. Calcium hydroxide, pH-neutralization and formulation of model self-adhesive resin cements. Dent. Mater. 2013; 29:413–418. [PubMed: 23398784]

36. Zhang N, Melo MAS, Antonucci JM, Lin NJ, Lin-Gibson S, Bai YX, Xu HHK. Novel dental cement to combat biofilms and reduce acids for orthodontic applications to avoid enamel demineralization. Materials. 2016; 9
37. Melinte V, Buruiana T, Chibac A, Mares M, Aldea H, Buruiana EC. New acid BisGMA analogs for dental adhesive applications with antimicrobial activity. Dent. Mater. 2016; 32:E314–E326. [PubMed: 27671467]
38. Farrugia C, Camilleri J. Antimicrobial properties of conventional restorative filling materials and advances in antimicrobial properties of composite resins and glass ionomer cements-a literature review. Dent. Mater. 2015; 31:E89–E99. [PubMed: 25582060]
39. Cocco AR, Maske TT, Lund RG, Moraes RR. The antibacterial and physicochemical properties of a one-step dental adhesive modified with potential antimicrobial agents. Int. J. Adhes. Adhes. 2016; 71:74–80.
40. Mehdawi I, Abou Neel EA, Valappil SP, Palmer G, Salih V, Pratten J, Spratt DA, Young AM. Development of remineralizing, antibacterial dental materials. Acta Biomater. 2009; 5:2525–2539. [PubMed: 19410530]
41. Tay FR, Pashley DH. Biomimetic remineralization of resin-bonded acid-etched dentin. J. Dent. Res. 2009; 88:719–724. [PubMed: 19734458]
42. Osorio R, Cabello I, Toledano M. Bioactivity of zinc-doped dental adhesives. J. Dent. 2014; 42:403–412. [PubMed: 24373854]
43. Taktak FF, Butun V. Synthesis and physical gels of pH- and thermo-responsive tertiary amine methacrylate based ABA triblock copolymers and drug release studies. Polymer. 2010; 51:3618–3626.
44. Van Overstraeten-Schlogel N, Shim YH, Tevel V, Piel G, Piette J, Dubois P, Raes M. Assessment of new biocompatible Poly(N-(morpholino)ethyl methacrylate)-based copolymers by transfection of immortalized keratinocytes. Drug Deliv. 2012; 19:112–122. [PubMed: 22239537]
45. Reschner A, Shim YH, Dubois P, Delvenne P, Evrard B, Marcelis L, Moucheron C, Kirsch-De Mesmaeker A, Defrancq E, Raes M, Piette J, Collard L, Piel G. Evaluation of a new biocompatible poly(N-(morpholino ethyl methacrylate)-based copolymer for the delivery of ruthenium oligonucleotides, targeting HPV16 E6 oncogene. J. Biomed. Nanotechnol. 2013; 9:1432–1440. [PubMed: 23926811]
46. Song LY, Ye Q, Ge XP, Misra A, Tamerler C, Spencer P. Self-strengthening hybrid dental adhesive via visible-light irradiation triple polymerization. RSC Adv. 2016; 6:52434–52447. [PubMed: 27774144]
47. Song LY, Ye Q, Ge XP, Misra A, Spencer P. Mimicking nature: self-strengthening properties in a dental adhesive. Acta Biomater. 2016; 35:138–152. [PubMed: 26883773]
48. Ge XP, Ye Q, Song LY, Laurence JS, Spencer P. Synthesis and evaluation of a novel co-initiator for dentin adhesives: polymerization kinetics and leachables study. JOM. 2015; 67:796–803. [PubMed: 26052187]
49. Guo X, Wang Y, Spencer P, Ye Q, Yao X. Effects of water content and initiator composition on photopolymerization of a model BisGMA/HEMA resin. Dent. Mater. 2008; 24:824–831. [PubMed: 18045679]
50. Ye Q, Park J, Topp E, Spencer P. Effect of photoinitiators on the in vitro performance of a dentin adhesive exposed to simulated oral environment. Dent. Mater. 2009; 25:452–458. [PubMed: 19027937]
51. Song LY, Ye Q, Ge XP, Misra A, Laurence JS, Berrie CL, Spencer P. Synthesis and evaluation of novel dental monomer with branched carboxyl acid group. J. Biomed. Mater. Res. Part B. 2014; 102:1473–1484.
52. Parthasarathy R, Misra A, Park J, Ye Q, Spencer P. Diffusion coefficients of water and leachables in methacrylate-based crosslinked polymers using absorption experiments. J. Mater. Sci.-Mater. Med. 2012; 23:1157–1172. [PubMed: 22430592]
53. Song LY, Ye Q, Ge XP, Misra A, Tamerler C, Spencer P. Probing the neutralization behavior of zwitterionic monomer-containing dental adhesive. Dent. Mater. 2017; 33:564–574. [PubMed: 28366234]

54. Park J, Ye Q, Topp EM, Misra A, Kieweg SL, Spencer P. Effect of photoinitiator system and water content on dynamic mechanical properties of a light-cured bisGMA/HEMA dental resin. J. Biomed. Mater. Res. Part A. 2010; 93A:1245–1251.
55. Ge XP, Ye Q, Song LY, Misra A, Spencer P. Synthesis and evaluation of novel siloxane-methacrylate monomers used as dentin adhesives. Dent. Mater. 2014; 30:1073–1087. [PubMed: 24993811]
56. Singh V, Misra A, Marangos O, Park J, Ye QA, Kieweg SL, Spencer P. Viscoelastic and fatigue properties of model methacrylate-based dentin adhesives. J. Biomed. Mater. Res. Part B. 2010; 95B:283–290.
57. Park JG, Ye Q, Topp EM, Misra A, Spencer P. Water sorption and dynamic mechanical properties of dentin adhesives with a urethane-based multifunctional methacrylate monomer. Dent. Mater. 2009; 25:1569–1575. [PubMed: 19709724]
58. Viljanen EK, Langer S, Skrifvars M, Vallittu PK. Analysis of residual monomers in dendritic methacrylate copolymers and composites by HPLC and headspace-GC/MS. Dent. Mater. 2006; 22:845–851. [PubMed: 16380160]
59. Brinker, CJ., Scherer, GW. Sol-gel Science: The Physics and Chemistry Sol-Gel Processing. Academic Press, INC; 1990.
60. Brinker CJ. Hydrolysis and condensation of silicates – effects on structure. J. Non-Cryst. Solids. 1988; 100:31–50.
61. Moreau JL, Sun LM, Chow LC, Xu HHK. Mechanical and acid neutralizing properties and bacteria inhibition of amorphous calcium phosphate dental nanocomposite. J. Biomed. Mater. Res. Part B. 2011; 98B:80–88.
62. Zhang D, Lepparanta O, Munukka E, Ylanen H, Viljanen MK, Eerola E, Hupa M, Hupa L. Antibacterial effects and dissolution behavior of six bioactive glasses. J. Biomed. Mater. Res. Part A. 2010; 93a:475–483.
63. Ge XP, Ye Q, Song LY, Spencer P, Laurence JS. Effect of crosslinking density of polymers and chemical structure of amine-containing monomers on the neutralization capacity of dentin adhesives. Dent. Mater. 2015; 31:1245–1253. [PubMed: 26342639]
64. Ge XP, Ye Q, Song LY, Laurence JS, Misra A, Spencer P. Probing the dual function of a novel tertiary amine compound in dentin adhesive formulations. Dent. Mater. 2016; 32:519–528. [PubMed: 26764171]
65. Sideridou ID, Karabela MM, Vouvoudi EC. Dynamic thermomechanical properties and sorption characteristics of two commercial light cured dental resin composites. Dent. Mater. 2008; 24:737–743. [PubMed: 17889316]
66. Mesquita RV, Geis-Gerstorfer J. Influence of temperature on the visco-elastic properties of direct and indirect dental composite resins. Dent. Mater. 2008; 24:623–632. [PubMed: 17826827]
67. Kowalewska A. Photoacid catalyzed sol-gel process. J. Mater. Chem. 2005; 15:4997–5006.
68. Croutxe-Barghorn C, Belon C, Chemtob A. Polymerization of hybrid sol-gel materials catalyzed by photoacids generation. J. Photopolym. Sci. Technol. 2010; 23:129–134.
69. De Paz H, Chemtob A, Croutxe-Barghorn C, Le Nouen D, Rigolet S. Insights into photoinduced sol-gel polymerization: an in situ infrared spectroscopy study. J. Phys. Chem. B. 2012; 116:5260–5268. [PubMed: 22486534]
70. Fonder MA, Lazarus GS, Cowan DA, Aronson-Cook B, Kohli AR, Mamelak AJ. Treating the chronic wound: a practical approach to the care of nonhealing wounds and wound care dressings. J. Am. Acad. Dermatol. 2008; 58:185–206. [PubMed: 18222318]
71. Teo AJT, Mishra A, Park I, Kim YJ, Park WT, Yoon YJ. Polymeric biomaterials for medical implants and devices. Acs Biomater. Sci. Eng. 2016; 2:454–472.
72. Khan F, Tanaka M, Ahmad SR. Fabrication of polymeric biomaterials: a strategy for tissue engineering and medical devices. J. Mater. Chem. B. 2015; 3:8224–8249.

Statement of Significance

The interfacial gaps between the restorative composite biomaterial and the tooth structure contributes to recurrent decay and failure of the composite restoration. The inability of the material to increase the pH at the composite/tooth interface facilitates the outgrowth of more cariogenic and aciduric bacteria.

This paper reports a novel, synthetic resin that provides buffering capability and autonomous strengthening characteristics. In this work, two amino functional silanes were synthesized and the effect of alkoxy substitutions on the photoacid-induced sol-gel reaction was investigated. We evaluated the neutralization capability (monitoring the pH of lactic acid solution) and the autonomous strengthening property (monitoring the mechanical properties of the hybrid copolymers under wet conditions and quantitatively analyzing the leachable species by HPLC). The novel resin investigated in this study offers the potential benefits of reducing the risk of recurrent decay and prolonging the functional lifetime of dental adhesives.

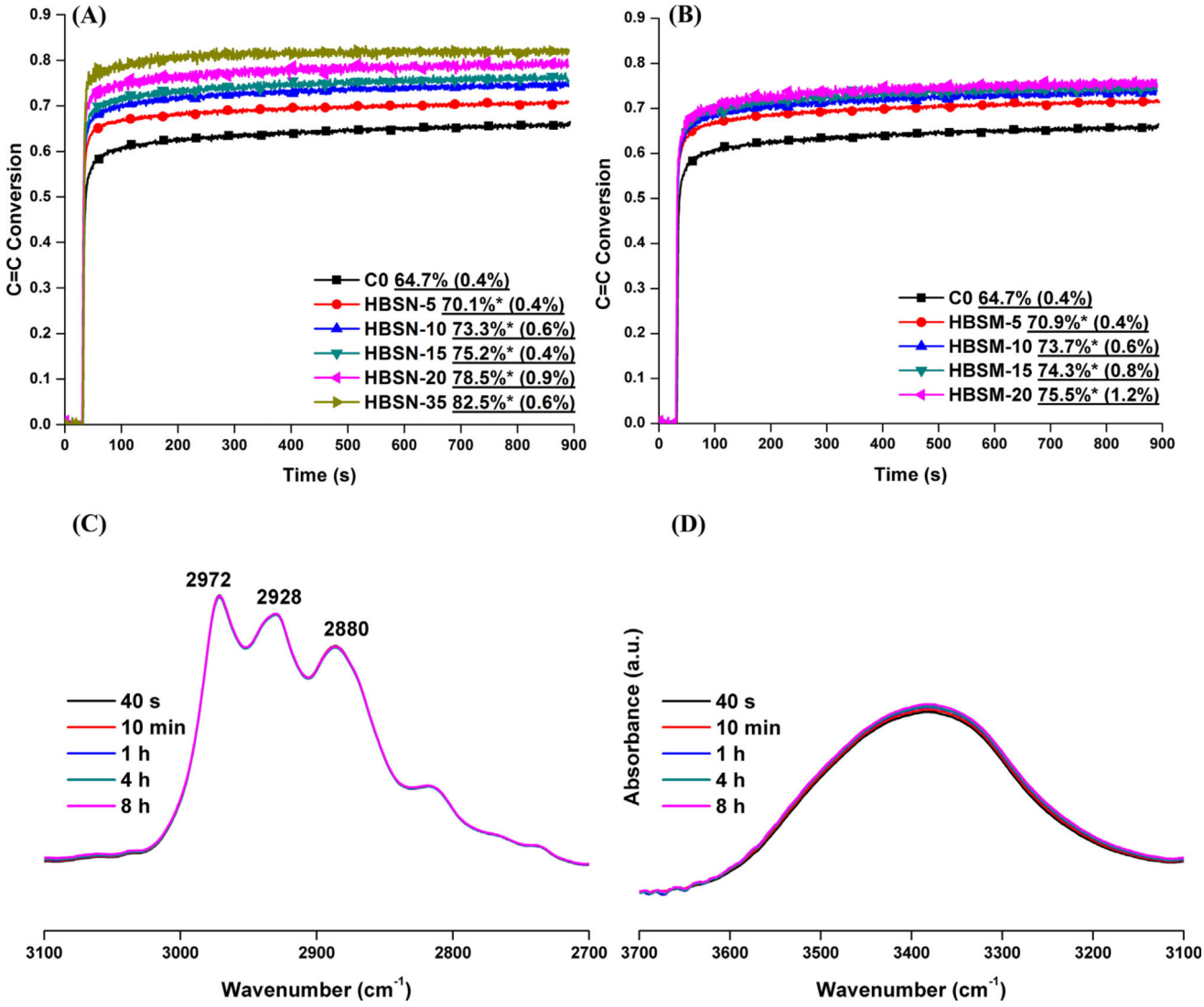

Fig. 1.

Real-time conversion of C=C bond of the C0 and experimental adhesives (A) SNE-containing formulations and (B) SNM-containing formulations, and FTIR characteristic peaks of SNE-containing formulation (HBSN-50) before and after visible-light irradiation, selective ranges of FTIR spectra for (C) alkoxyl group and (D) hydrogen bond. (The adhesives were light-cured for 40 s at 23 ± 2 °C using a commercial visible light lamp: Spectrum® 800, Dentsply, Milford, DE. Intensity is 550 mW/cm^2.)

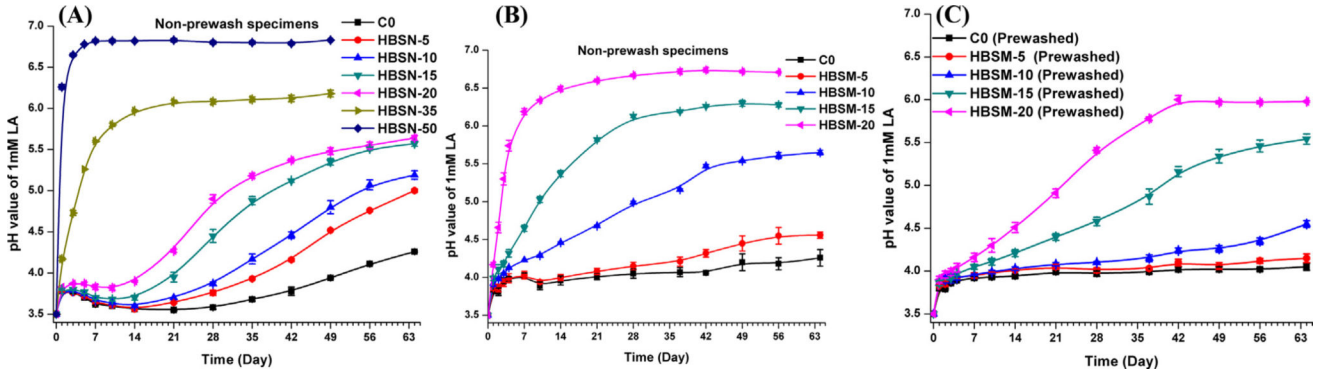

Fig. 2.

Plots of the pH values of 1 mM LA solution containing the C0 and experimental specimens versus storage time, (A) HBSN specimens without prewash, (B) HBSM specimens without prewash, and (C) prewashed and hydrated HBSM specimens. (Volume of LA is 2 mL, initial pH is 3.50, and temperature is 23 ± 2 °C).

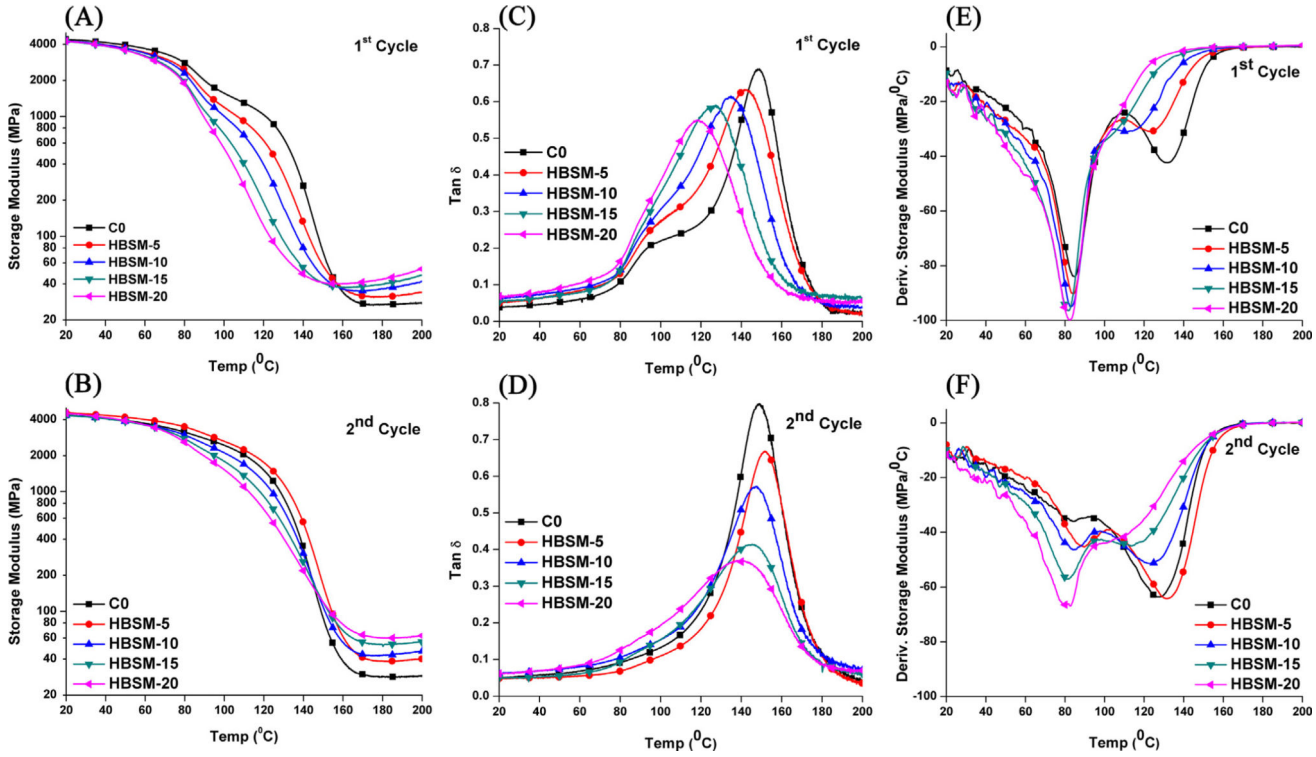

Fig. 3.

Representative storage modulus (A and B), derivative storage modulus (C and D), and tan δ (E and F) vs. temperature curves of the SNM-containing specimens in dry conditions for the first DMA cycle (Top) and second DMA cycle (Bottom).

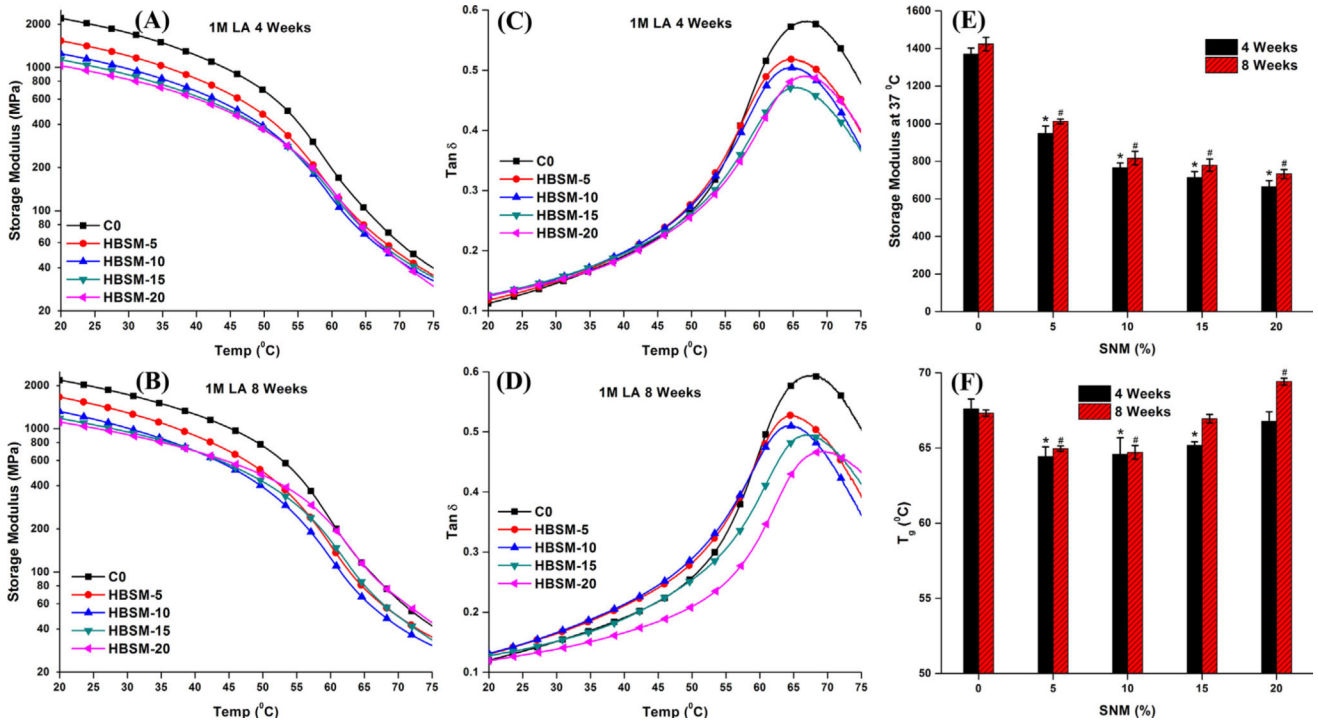

Fig. 4.

Representative storage modulus (A and B) and tan δ (C and D) vs. temperature curves, the storage moduli at 37 °C bar figure (E), and T_g values (F) of the C0 and HBSM experimental copolymers soaked in 1 M LA solution for 4 and 8 weeks (T_g was obtained from the position of maximum peak on the tan δ vs. temperature plots, * # Significantly ($p < .05$) different from the control soaked for 4 or 8 weeks in LA solution, respectively.

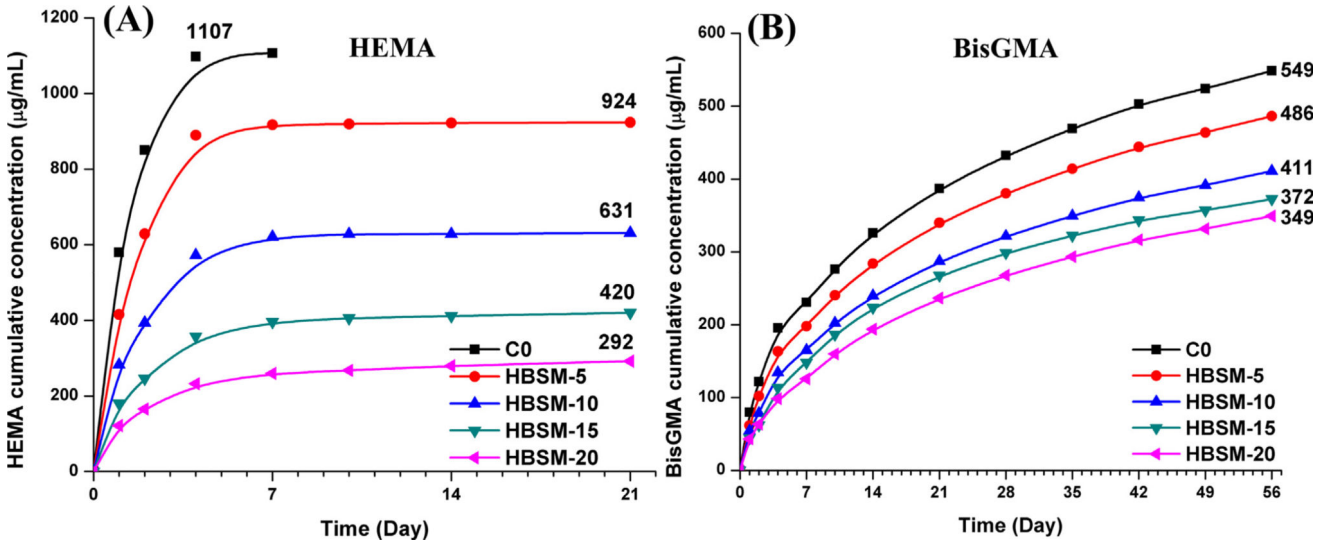

Fig. 5.

Cumulative monomers release from the SNM-containing copolymers as a function of incubation time in ethanol: (A) HEMA and (B) BisGMA.

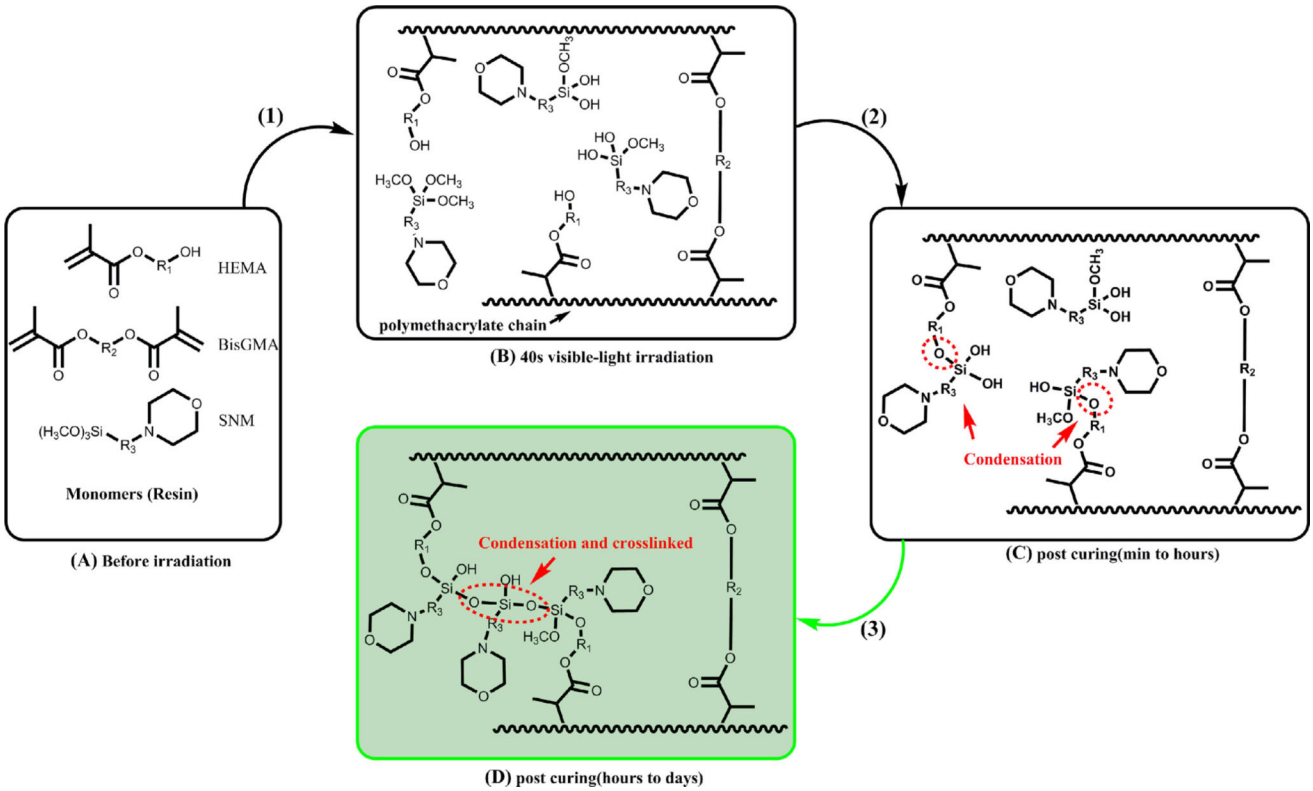

Scheme 1.

Proposed polymethacrylate-based matrix network structure and the self-strengthening process of SNM-containing adhesive. (A) Neat resin (before irradiation); (B) Polymethacrylate-based network formed by free radical polymerization (during 40 s visible-light irradiation); (C) limited photoacid-induced sol-gel reaction after 40 s irradiation (minutes to hours); (D) hybrid polymethacrylate/polysiloxane crosslinked network (few hours to days).

Table 1

Results of Degree of Conversion and Maximum Polymerization Rate of Formulations.

Run	HEMA/BisGMA (wt%)[a]	SNE (wt%)	SNM (wt%)	W_{wm} (wt%)	DC[b] (%)	$\frac{R_p^{max}}{[M]} \times 100(1/s)$
C0	100	0	0	10.5(0.1)	64.8 (0.4)	20.6(1.2)
HBSN-5	95	5	/	10.8(0.1)	70.1*(0.4)	26.7(0.4)
HBSN-10	90	10	/	11.1(0.1)	73.3*(0.6)	27.3(1.2)
HBSN-15	85	15	/	11.3(0.1)	75.2*(0.4)	26.0(0.3)
HBSN-20	80	20	/	11.5(0.0)	78.5*(0.9)	25.9(0.4)
HBSN-35	65	35	/	12.5(0.1)	82.5*(0.6)	23.0(0.8)
HBSN-50	50	50	/	14.2(0.0)	75.1*(0.8)	21.9(1.2)
HBSM-5	95	/	5	10.5(0.2)	70.9*(0.4)	28.0(2.2)
HBSM-10	90	/	10	10.7(0.3)	73.7*(0.6)	33.2(1.8)
HBSM-15	85	/	15	11.0(0.1)	74.3*(0.3)	31.5(2.2)
HBSM-20	80	/	20	11.4(0.2)	75.5*(0.3)	30.7(2.3)

[a] The resin was mixed with HEMA/BisGMA in the ratio of 45/55 (w/w).

[b] Degree of conversion of C=C bond.

* Significantly ($p < .05$) different from the control (C0). The value in the () is the standard deviation.